Cellulose-based materials in tailoring a novel defective titanium-carbon-phosphorus hybrid composites for highly efficient photocatalytic activity

Hesham Hamad, Mahmoud Samy, Esther Bailón-García, Igor Bezverkhyy, Magdalena Skompska, Francisco Carrasco-Marín, Agustín F Pérez-Cadenas

International Journal of Biological Macromolecules 270 (2024) 132304

Contents lists available at ScienceDirect

International Journal of Biological Macromolecules

journal homepage: www.elsevier.com/locate/ijbiomac

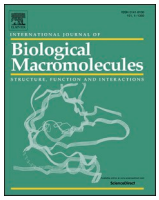

Cellulose-based materials in tailoring a novel defective titanium-carbon-phosphorus hybrid composites for highly efficient photocatalytic activity

Hesham Hamad [a,b,c,*], Mahmoud Samy [d], Esther Bailón-García [a], Igor Bezverkhyy [e], Magdalena Skompska [c], Francisco Carrasco-Marín [a], Agustín F. Pérez-Cadenas [a]

[a] UGR-Carbon, Materiales Polifuncionales Basados en Carbono, Departamento de Química Inorgánica, Facultad de Ciencias - Unidad de Excelencia Química Aplicada a Biomedicina y Medioambiente Universidad de Granada (UEQ-UGR), 18071 Granada, Spain
[b] Fabrication Technology Research Department, Advanced Technology and New Materials Research Institute (ATNMRI), City of Scientific Research and Technological Applications (SRTA-City), New Borg El-Arab City 21934, Alexandria, Egypt
[c] Laboratory of Electrochemistry, Faculty of Chemistry, University of Warsaw, Pasteur 1, 02-093 Warsaw, Poland
[d] Department of Public Works Engineering, Faculty of Engineering, Mansoura University, Mansoura 35516, Egypt
[e] Laboratoire Interdisciplinaire Carnot de Bourgogne, UMR 6303 CNRS-Université de Bourgogne, 9 Avenue Alain Savary, BP 47870-21078 Dijon Cedex, France

ARTICLE INFO

Keywords:
Coloured carbon-titanium-phosphorous composites
Cellulose functionalization
Photocatalysis

ABSTRACT

Until now, black titania has attracted much interest as a potential photocatalyst. In this contribution, we report the first demonstration of the effective strategy to fundamentally improve the photocatalytic performance using a novel sustainable defective titanium-carbon-phosphorous (TCPH) hybrid nanocomposite. The prepared TCPH was used for photocatalytic degradation of the main organic pollutants, which is methyl orange (MO) dye. The physico-chemical properties of as-prepared samples were characterized by various techniques to observe the transformations after carbonization and the interaction between different composite phases. The existence of Ti^{+3} and oxygen vacancies at the surface, and a notable increase in surface area, are all demonstrated by TCPH, together with the distinct core-shell structure. These unique properties exhibit excellent photocatalytic performance due to the boosted charge transport and separation. The highest degradation efficiency of methyl orange (MO) was attained in the case of TCPH when compared with titanium-cellulose-phosphorous (TCeP) and titanium-carbon-phosphorous (TCPN). Accordingly, the highest degradation efficiency was achieved by applying the optimal operational conditions of 1 g/L of TCPH catalyst, 10 mg/L of MO, pH of 7 and the temperature at 25 ± 3 °C after 3 min under LED lamp (365 nm) with light intensity 100 mW/cm^2. The degradation mechanism was investigated, and the trapping tests showed the dominance of hydroxyl radicals in the degradation of MO. TCPH showed high stability under a long period of operation in five consecutive cycles, which renders the highly promising on an industrial scale. The fabrication of highly active defective titanium-carbon-phosphorous opens new opportunities in various areas, including water splitting, and CO_2 reduction.

1. Introduction

Water sources receive large volumes of industrial effluents containing emerging micropollutants (EMPs) such as dyes, phenols, antibiotics, and pesticides. The discharge of EMPs to water streams without proper purification has a ferocious impact on the aquatic environment and human health [1]. Hence, fixing these problems and detoxifying wastewater are urgently requested. The need for low-cost and highly efficient water treatment strategies is solving these pollution problems from natural sources [2].

With today's strict requirements for efficient degradation of EMPs, heterogeneous photocatalysis is seen as a promising eco-friendly approach due to its ability to utilize solar light to generate radicals which decreases the energy consumption and consequently reduces the treatment cost [3,4]. Moreover, no sludge is produced during the degradation by the photocatalysis process [5]. About 70 % of the dye

* Corresponding author at: UGR-Carbon, Materiales Polifuncionales Basados en Carbono, Departamento de Química Inorgánica, Facultad de Ciencias - Unidad de Excelencia Química Aplicada a Biomedicina y Medioambiente Universidad de Granada (UEQ-UGR), 18071 Granada, Spain.
E-mail addresses: inv.heshamaterials@ugr.es, heshamaterials@hotmail.com (H. Hamad).

https://doi.org/10.1016/j.ijbiomac.2024.132304
Received 16 March 2024; Received in revised form 7 May 2024; Accepted 10 May 2024
Available online 12 May 2024

family was made up of complexes that contained azo, with methyl orange (MO) serving as a model complex for photodegradation. Titanium dioxide (TiO_2) is commonly employed in the photodegradation of EMPs due to its high stability, insolubility, cost-effectiveness, abundance, and unique catalytic performance [6,7]. However, wide bandgap and fast recombination of electron-hole pairs obstruct the way towards the large-scale application of the photocatalysis process using TiO_2 [8,9]. The wide bandgap of TiO_2 restrains the exploitation of solar light energy and makes the excitation only take place under UV light which constitutes only 5 % of solar energy [10]. On the other hand, fast concourse between the charge carriers results in the decrease of generated reactive radicals which reduces the degradation performance [11]. The decrease of bandgap and retard of recombination rate can improve the degradation performance and extend the absorption to visible light region. Many efforts have been dedicated to tackle these limitations such as doping bare photocatalysts (TiO_2) with metals (Zr, Fe, Zn) or/and non-metals (N, P, S) and construction of composites of pure metal oxide and materials that can accept electrons such as carbonaceous materials (carbon nanotubes, nanocarbon, graphene and fullerenes) and semiconductors (ZnO, ZrO_2, CdS and $BiVO_4$) [12–16]. However, the aforementioned modifications require the usage of expensive and harmful chemicals that inhibit the mass production of synthesized photocatalysts and their large-scale application in environmental remediation [17].

Cellulose is a biopolymer that can be extracted from plants, and it is characterized by abundance, low-cost, biodegradability, and carbon-rich content (44.4 % carbon) [18]. Cellulose can be used as a supporting material for pure TiO_2 which leads to the increase of adsorption affinity towards target pollutants, chemical stability, active sites and surface area [2,19]. Because it has provided a variety of active sites for the surface reactions at wide potential applications, particularly in the field of photocatalysis, the control of the synthesis of hierarchical structure of nano and micromaterials (i.e., cellulose/TiO_2) is promising and appealing [20]. Additionally, it has been suggested that adding impurities into TiO_2 lattices will increase the photocatalytic activity because it prevents charge recombination, improves interfacial charge transfer, and adds extra energy levels and defects to the material's electronic and textural, respectively [21]. The most intriguing kind of integration entails surface alterations through doping with an anionic ion, such as phosphate. A P^{5+} ion is a different type of dopant that has empty 3D states that are positioned in the lower energy range of TiO_2's valence band [22]. Due to the increase in surface acidity, thermal stability, and subsequent promotion of rapid redox reaction by the fast formation of hydroxyl radicals, the phosphorylation of TiO_2 has gained a lot of attention recently [7].

In our previous work, cellulose was first dissolved in phosphoric acid (H_3PO_4) before TiO_2 impregnation to improve the TiO_2 dispersion and increase TiO_2 loading on the cellulose surface [21]. Additionally, acid treatment can contribute to the introduction of new oxygen and phosphorous-containing functional groups on cellulose surface which can improve the adsorption performance [3]. The TiO_2/cellulose (treated with phosphoric acid) composite was carbonized under N_2 to prepare titanium-carbon-phosphorous composite due to the high carbon content from cellulose and improve the porosity of the composite. The presence of carbon can improve the adsorption ability of the composite, suppress the recombination between charge carriers and boost the absorption under visible light [13,23,24]. The interaction between Ti and carbon plays an important role in tuning the absorption to a wide range of solar light, decreasing the rate of recombination, boosting the adsorption characteristics, as well as solving the problem of aggregation of TiO_2 during the synthesis [25]. Moreover, the usage of cellulose as a carbon source can reduce the total cost of the composite which paves the way for the scalable production and full-scale application of photocatalysis process.

Another alternative for boosting the photocatalytic activity is the modification of TiO_2 by transforming Ti^{4+} to Ti^{3+} which produces so called black titania, having black or colourful appearances [26]. Additionally, this material is featured by the high electron mobility and narrow bandgap (around 1.5 eV), so it can absorb large portion (nearly 83 %) of the solar light and generate more radicals [26–28].

The purpose of our work is to prepare the high value-added novel titanium-carbon-phosphorus composite for the photocatalytic degradation of methyl orange (MO) dye, one of the major organic pollutants. To the best of our knowledge, the fabrication of defective coloured titanium-carbon-phosphorus composite (TCPH) and its photocatalytic performance has not been reported so far. The synthetic strategy for TCPH consists of facile in situ sol-gel method via the dissolution of microcrystalline cellulose by phosphoric acid followed by impregnation of titania precursor with dissolved cellulose and subsequent carbonization at various environments (N_2 and H_2). The simplicity of preparation and relatively low cost may encourage the production of hybrid materials continually for various industrial applications. The impact of carbonization and hydrogenation treatment on the structural, morphological, textural, thermal stability, optical properties, and interaction between phases was investigated to evaluate the synergy between the multiple components and their effect on the enhancement of photocatalytic reactivity. Based on this, a possible mechanism of the photocatalytic degradation of MO dye using the hybrid composite is proposed. The major reactive oxygen species were determined using trapping experiments. The stability of prepared materials was evaluated under successive cycles. We introduce new insights that will be appropriate for the design of coloured titania nanocomposite photocatalysts benefiting from a slow rate of electron/hole recombination after introducing oxygen vacancies and core-shell structure for highly efficient the photocatalytic performance.

2. Materials and methods

2.1. Chemicals

Microcrystalline cellulose (MCC, 99 %), titanium (IV) tetra isopropoxide (TTIP, $C_{12}H_{28}O_4Ti$, 99 %) and ortho-phosphoric acid (H_3PO_4, 85 % *w*/w) were purchased from Merck (Germany). Nitric acid (HNO_3, 70 % w/w), heptane (C_7H_{16}, 95 %), acetone (C_3H_6O, 99 %), ethylenediaminetetraacetic acid (EDTA, $C_{10}H_{16}N_2O_8$, 97 %), methanol (MA, CH_3OH, 95 %), benzoquinone (BQ, $C_6H_4O_2$, 95 %) and ethanol (C_2H_5OH, 97 %) were purchased from VWR chemicals (Belgium). Methyl Orange (MO, $C_{14}H_{14}N_3NaO_3S$) was procured from Acros Organics (Belgium). The water used was purified by Millipore instrument. White titania, TiO_2 anatase from Sigma-Aldrich, was used as reference material.

2.2. Synthesis of coloured titanium-carbon-phosphorous hybrid nanocomposites

Core-shell defective coloured titanium-carbon-phosphorous (TCPH) hybrid nanocomposite were prepared by coating of titanium-cellulose-phosphorous with disordered shell. The overall procedure for the synthesis of core-shell structured hybrid nanocomposite is presented through three determinant steps as follows:

(i) Dissolution of microcrystalline cellulose using acid hydrolysis; 10 g of MCC was added to 50 mL of distilled water and the solution was stirred at 50 °C for 15 min. Subsequently, the dissolution of MCC was performed by adding 10 mL of H_3PO_4 acid in a drop-wise manner to MCC slurry and stirring for 24 h [4].

(ii) TiO_2 impregnation by sol-gel method; titanium precursor, TTIP, was dissolved in 150 mL of heptane and stirred at 50 °C, then specific volume of Ti solution was added to MCC solution with a mass ratio of 1:6 for cellulose and titanium dioxide, respectively. Owing to the hydrolysis of TTIP, a solid suspension was formed, and the suspension was heated and stirred at 60 °C for 24 h. Then, the suspension was filtered followed by washing with ethanol,

distilled water, and acetone and drying at 120 °C in an oven to remove water and obtain TiP_2O_7 instead of $Ti(HPO_4)_2{\cdot}H_2O$ [2]. The obtained material was referred as TCeP.

(iii) Defective coloured titanium-carbon-phosphorous composites; the previous preparation procedures were followed (besides the carbonization of titanium-cellulose-phosphorous composite) in a tubular furnace under N_2 atmosphere at 500 °C at 10 °C/min. To prepare defective coloured titanium-carbon-phosphorus nanocomposite, the process was conducted under H_2 flow.

In this work, three nanocomposites were synthesized with the abbreviations of TCeP, TCPN and TCPH which refer to titanium dioxide (T), cellulose (Ce), Carbon (C), phosphorous (P), N_2 (N), H_2 (H), respectively.

2.3. Characterization techniques and photocatalytic tests

The details of the characterization techniques and the photocatalytic tests are given in supporting information S1 and S2, respectively.

3. Results and discussion

In previous work, the treatment of cellulose with phosphoric acid led to improving the dispersion of the Ti-active phase on the cellulose support and functionalizing it directly with phosphorous-containing groups, resulting in carbon-phosphorous-Ti composites [2]. This is due to the strong inter- and intra-molecular hydrogen bonds in cellulose that refer to the abundant hydroxyl groups already existing in the inner cellulose structure. The activity of the fabricated hybrid nanocomposite of carbon-titanium-phosphorous depends on the dispersion of active sites, its interaction of cellulose support, surface area, and carbonization environments (N_2 or H_2). It is well known that the presence of Ti^{+3} and oxygen vacancies favour the photocatalytic activity in the visible range due to the minimization of electron-hole recombination. Therefore, in the present work, for the first time, we explain the synergistic interaction between multiple components of defective coloured titanium-carbon-phosphorous composites. The results of the physicochemical characterization, photocatalytic performance, and mechanistic insights are shown and discussed below.

3.1. Physicochemical characteristics of the prepared hybrid nanocomposites

The carbonization process of commercial MCC as raw materials and a precursor of carbonaceous materials, acid-treated cellulose with phosphoric acid (CeP), and its impregnated with titania (TCeP) were investigated by TGA under N_2 flow, indicating the significant changes on the thermal stability of cellulose before and after treatment with acid and/or impregnated with titania (Fig. 1). The weight loss took place in single step in the case of MCC at nearly 300 °C which affirmed the absence of hemicellulose and lignin [29]. For CeP, the weight loss occurred in two steps. The first weight loss was at nearly 300 °C due to the dehydration and the decomposition of carboxylic acids and anhydrides to CO_2. The weight loss in the range from 300 to 750 °C was lower compared to MCC due to the distribution of functional groups on the surface. The second weight loss at about 750 °C was mainly due to the reduction of phosphate groups by cellulose leading to the increase of cellulose gasification [2]. The change of weight loss in the case of TCeP was due to the chemical bonds formed between Ti precursor and cellulose and/or carbon. The weight loss was a bit higher at a temperature of nearly 300 °C due to the decomposition of organic precursors. However, the weight loss was lower by increasing the temperature above 300 °C compared to MCC and CeP which confirmed the thermal stability due to the interaction between cellulose oxygenated surface and Ti phase.

The band gap was estimated as shown in Fig. 2 by plotting $(F(R)\,h\nu)^2$ versus $h\nu$, where F(R) and $h\nu$ are the functions of reflectance and photon energy, respectively. The band gap is the intersection of the extension of the linear portion in Fig. 2 with the x-axis. The band gap of TCeP, TCPN and TCPH was 3.88, 3.70 and 3.13 eV, respectively. The band gap of TCeP was higher than that of pure TiO_2 (3–3.2 eV) due to the formed amorphous TiP_2O_7 [2]. The band gap decreased in the case of TCPN due to the interaction between carbon and Ti phases during carbonization. In the case of TCPH, the bandgap was narrower, and the enhanced visible light absorption is due to the effective reduction of Ti^{4+} ions into Ti^{3+} and oxygen vacancies that could be formed during hydrogenation [30].

The presence of Ti^{3+} and oxygen vacancies was further confirmed by XPS analysis. The XPS spectra showing the transformations and chemical interactions between cellulose, phosphorous and Ti phases are presented in Fig. 3. Also, the chemical composition and the variation of the nature of the surface functional groups are summarized in Table 1. The strong functionalization of TCeP sample is correlated to the high phosphorous content. The reduction of oxygen content of TCPN and TCPH (i.e., 43.3 and 33.6, respectively) due to the thermal decomposition of phosphorous and oxygen functionalities, taking into consideration the hydrogen environment leads to the decrease the functionalities as compared to nitrogen environment [2]. On the other hand, the thermal stability is increased by the increase of the amount of phosphate containing-groups and concurrently with the increase the oxygen-containing groups.

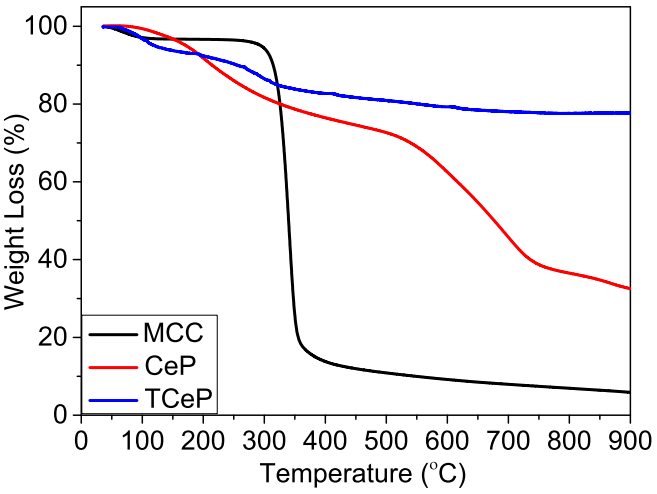

Fig. 1. TGA of MCC, CeP and TCeP.

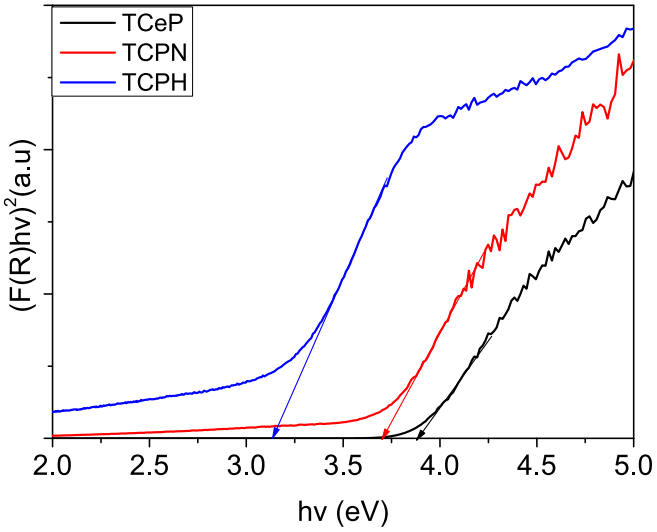

Fig. 2. Diffuse reflectance spectra of TCeP, TCPN, and TCPH.

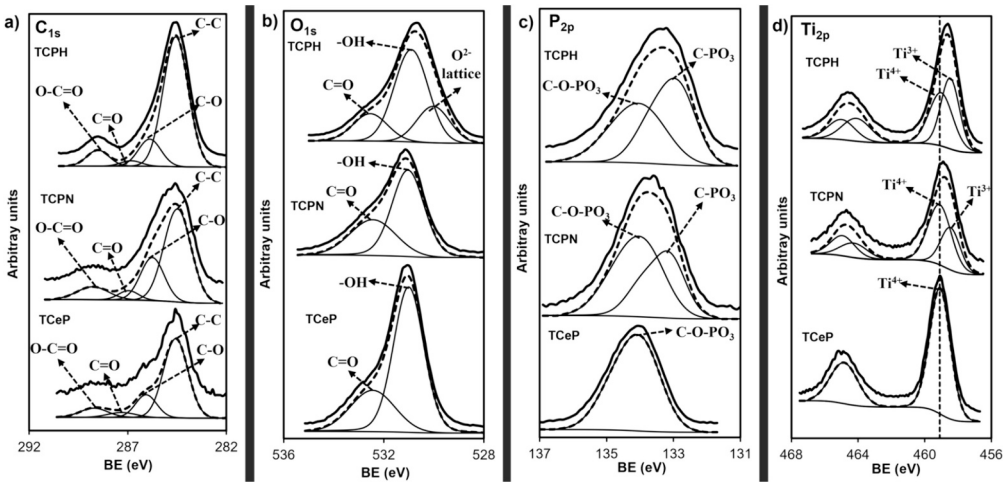

Fig. 3. XPS spectra of (a) C_{1s}, (b) O_{1s}, (C) P_{2p} and (d) Ti_{2p} of TCeP, TCPN and TCPH.

Table 1
The surface concentration and species percentage of the prepared titania hybrid composites obtained at different atmosphere (N_2 or H_2).

Sample	C	O	P	Ti	P_{2p} (%)		Ti_{2p} (%)	
	(wt%)				C-O-PO_3	C-PO_3	Ti^{3+}	Ti^{+4}
TCeP	8.5	47.7	26.6	17.3	100	0	0	100
TCPN	21.2	43.4	21.7	13.7	58	42	37	63
TCPH	34.0	33.6	17.0	16.7	46	54	50	50

The peaks at around 284.6 eV are attributed to C—C (C_{1s}) in the case of TCeP, TCPN and TCPH as shown in Fig. 3a. As the result of hydrogenation at 500 °C, the percentage of carbon is increased from 8.5 % in case of TCeP to 21.2 and 34.0 % for TCPN and TCPH, respectively, indicating that the conversion of cellulose to carbon after thermal treatment (Table 1). The peaks at binding energies higher than 284.6 eV are allocated to oxygenated surface and carboxyl groups (O-C=O, C=O and C—O) as shown in Fig. 3a. The peaks at around 531.0 and 532.4 eV in Fig. 3b are ascribed to oxygen with a single bond and to oxygen (O_{1s}) with double bonds (e.g., carbonyl and carboxyl groups), respectively. Moreover, the peaks of O_{1s} could be due to Ti—O and Ti-OH bonds. The hydrogenation could cleavage Ti—O bonds to Ti—H and O—H bonds resulting in the presence of hydroxyl groups on the surface. In TCPH, there is a new peak at 530.0 eV that refers to the surface oxygen vacancies with concentration of 23 %. The existence of oxygen vacancies is crucial for photocatalytic activity, resulting the TCPH has more advantage than TCPN. The carbonization in N_2 or H_2 led to the progressive reduction of TCPN and TCPH, respectively, since the oxygen decreased (i.e., 47.7, 43.4, and 33.6 % for TCeP, TCPN and TCPH, respectively) due to the thermal decomposition of some oxygen and/or phosphorous functionalities, which were evolved as CO_x. In addition, the amount of oxygen decreased more in TCPH than in TCPN, which confirmed that the reduction of TCPH is effectively higher than TCPN (Table 1). In TCeP, there is one peak at 133.9 eV attributed to the pentavalent tetra-coordinated phosphorous in phosphate or polyphosphates (C-O-PO_3) groups, i.e. $(CO)_3PO$, $(CO)_2PO_2$ and $(CO)PO_3$ which affirmed the presence of oxygen and phosphorous-containing groups after the treatment by H_3PO_4 as given in Fig. 3c [31]. After heat treatment, the peak was deconvoluted using two doublet peaks. The peak at 133.1 in TCPN (annealed in nitrogen atmosphere), and the peak at 132.8 eV for TCPH (in hydrogen atmosphere), are attributed to P atom bonded to one C atom and three or O atoms (i.e.; C–PO_3 group [32,33]. The shift indicating the reduction of the oxidation states of the phosphorous groups (P—O).

The peak at around 459.1 eV in the case of TCeP, TCPN and TCPH is ascribed to Ti^{+4} (Ti_{2p}) confirming the interaction between Ti precursor and carbonized cellulose (Fig. 3(d)). In the case of TCPH, another peak at around 458.5 eV is imputed to Ti^{+3} of black titania due to the hydrogenation under high temperature. The spectra of Ti $_{2p}$ in TCPH and TCPN is shifted to lower BE values, because of the mixture of Ti^{4+} and Ti^{+3} that denoting the impact of the carbonization at hydrogen environment on the nature of Ti and P phases. Moreover, the % of Ti^{+3} increases with the treatment of hydrogen (i.e., 37 vs 50 % for TCPN and TCPH, respectively (Table 1)), which corroborates the results obtained from diffuse reflectance analysis (Fig. 2).

The different interactions between TiO_2 and functionalized cellulose with phosphoric acid at various carbonization environments are clarified by various structures in Fig. 4a. It shows the XRD patterns of TCeP and TCPH indicating the amorphous structure of the synthesized materials, as phosphorous-containing groups might inhibit the growth of crystals and Ti precursor could react with phosphate forming TiP_2O_7 crystalline phase [7]. On the other hand, the carbonization in the N_2 atmosphere leads to avoiding the role of phosphate groups and results in the formation of the anatase structure of TiO_2 [21]. The diffraction peaks at 25.4°, 37.9°, 47.9°, 54.2°, 55.6°, 62.9°, and 68.5° in the case of TCPN are attributed to (101), (004), (200), (105), (211), (204) and (116) diffraction planes of anatase TiO_2 according to (JCPDS No. 21-1272) [34]. The peaks corresponding to TiP_2O_7 were not observed in the case of TCPN and TCPH due to the TiP_2O_7 was formed at higher temperatures (<750 °C). Another note is related to the crystallinity decreases by the reduction of titania [35]. As a result, the decrease of the crystallinity is obvious in sample TCPH. There were no unique peaks for the cellulose or carbon due to the interference between the components' peaks confirming the excellent interaction between the phases.

The textural characteristics of samples were analysed by N_2 adsorption-desorption isotherms of TCeP, TCPN and TCPH in Fig. 4b and c and the data are mentioned in Table 2. The surface area was 52, 45 and 213 m^2/g in the case of TCeP, TCPN and TCPH, respectively. The changes in surface area were due to the variation in morphology and porosity of the synthesized nanomaterials. The isotherms in Fig. 4c are of IV type, indicating the mesoporous character. A clear hysteresis cycle is observed in all samples at $P/P_o > 0.4$ due to N_2 condensation which affirmed the existence of high mesoporous and low microporous volumes. However, a significant increase in the surface area of TCPH, indicating the development of microporosity and mesoporosity (Table 2), thus, the hydrogenation improves the textural properties. The amorphous TCPH that observed in XRD typically shows the higher BET surface area than the crystalline TCPN [36]. The broad pore size distribution, high pore volume in the case of TCPH suggested its high photocatalytic and reusability performance. The reduction process

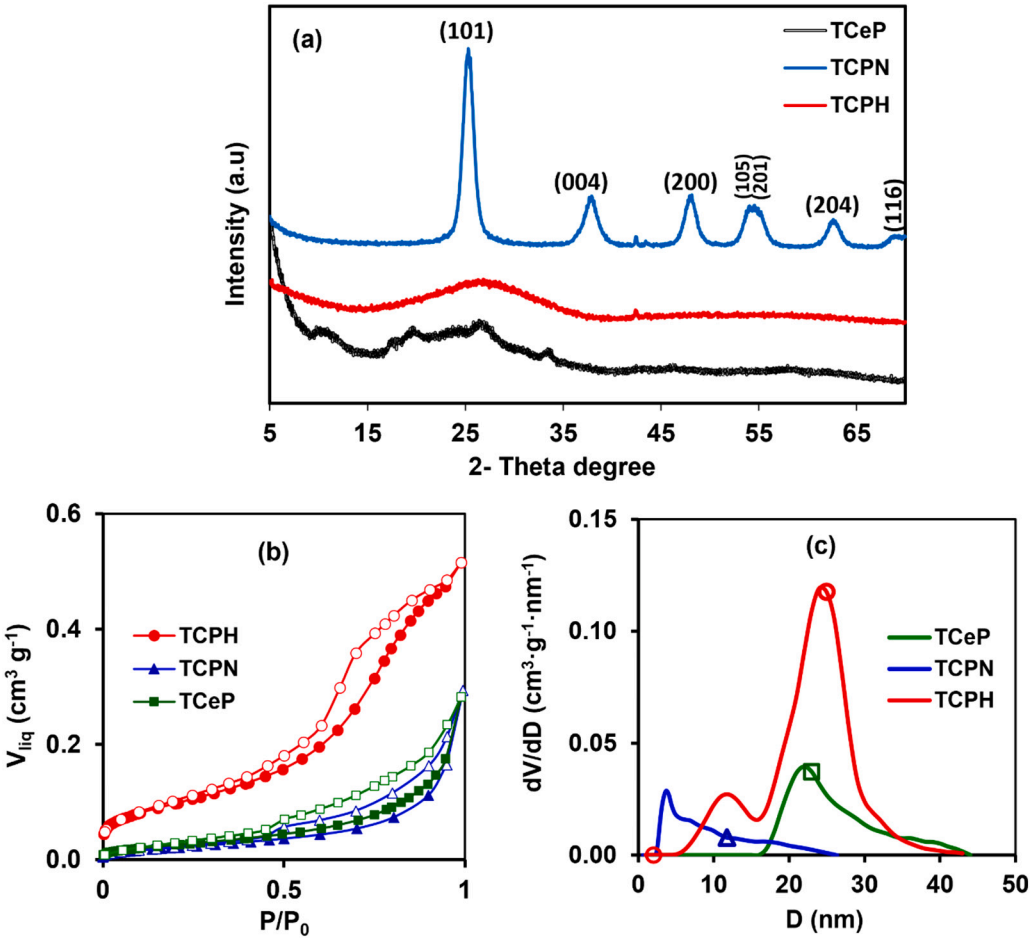

Fig. 4. (a) XRD pattern, (b) adsorption-desorption isotherm, and (c) pore size distribution of TCeP, TCPN and TCPH.

Table 2
Textural characteristics of TCeP, TCPN and TCPH.

Sample	S_{BET} (m^2/g)	S_{DFT} (m^2/g)	W_0 (cm^3/g)	L_0 (nm)	$V_{0.95}$ (cm^3/g)	V_{meso} (cm^3/g)
TCeP	52	70	0.02	1.67	0.17	0.16
TCPN	45	58	0.01	1.44	0.16	0.15
TCPH	213	208	0.08	1.52	0.47	0.40

improves the pore structure and surface area of TCPH (Table 2), and subsequently could boost the photocatalytic performance.

The morphological properties of the prepared samples were analysed by SEM, TEM, and HR-TEM. SEM images of TCeP, TCPN and TCPH are depicted in Fig. 5a, b and c. Fig. 5a shows the various morphology of TCeP due to the acid treatment of the cellulose confirming the excellent distribution of TiO_2 on cellulose surface and the porous structure were formed by the elongated particles of raw cellulose fibers. After the carbonization by N_2 at 500 °C as shown in Fig. 5b, the cellulose structure became more compact with clear microfibers and the particles with round shape were observed owing to the formation of TiO_2 on cellulose surface (Fig. 5b). The morphology of TCPH in Fig. 5c was mainly round shaped due to the formed black titania affirming the uniform distribution of TiO_2 on the formed carbon matrix produced after the carbonization of cellulose. Moreover, particles appeared in granules owing to the formation of the TiP_2O_7 crystalline phase during carbonization. TEM image in Fig. 5d and e shows the unique core-shell structure with a highly disordered surface layer coating a crystalline core of titania which agrees with our previous work [26]. The high-resolution TEM image is in Fig. 5f showed a confirmation of the core structure. The EDS pattern is in Fig. S1a indicated the presence of Ti, C, O and P with high atomic and weight ratios confirming the excellent impregnation of TiP_2O_7 on the carbon surface and the functionalization with phosphorus, in agreement with results previously reported [2]. Fig. S1 b, c, d, and f shows the EDS elemental mapping of TCPH and reaffirmed the chemical composition.

3.2. Photocatalytic activity

The photocatalytic performance of TCeP, TCPN, and TCPH was evaluated towards the degradation of MO dye under the illumination of an LED lamp with a wavelength of 365 nm (Fig. 6a). Before photocatalysis, the catalyst was saturated with MO dye in the dark to avoid the effect of adsorption. The initial MO concentration of 10 mg/L, pH 7 and light intensity of 100 mW/cm^2. The degradation percentages of MO were 62 %, 80 % and 99.1 % in the case of TCeP, TCPN and TCPH, respectively. Despite the higher surface area and mesoporosity of TCeP than TCPN, the degradation efficiency of MO in the case of TCPN was higher than that of TCeP due to the formed carbon after the carbonization of cellulose. The interaction between carbon and TiO_2 could result in the decrease of bandgap as explained in the characterization section. Moreover, carbon could act as an electron acceptor which resulted in suppressing the recombination between charge carriers and consequently the degradation efficiency was ameliorated [13]. TCPH exhibited the highest degradation performance due to the high surface area and mesoporosity which increased the composite's affinity to MO. Moreover, the fabricated coloured TCPH and carbon after the hydrogenation of TCeP could decrease the bandgap and solve the problem of electron/hole recombination which contributed to the increase of the

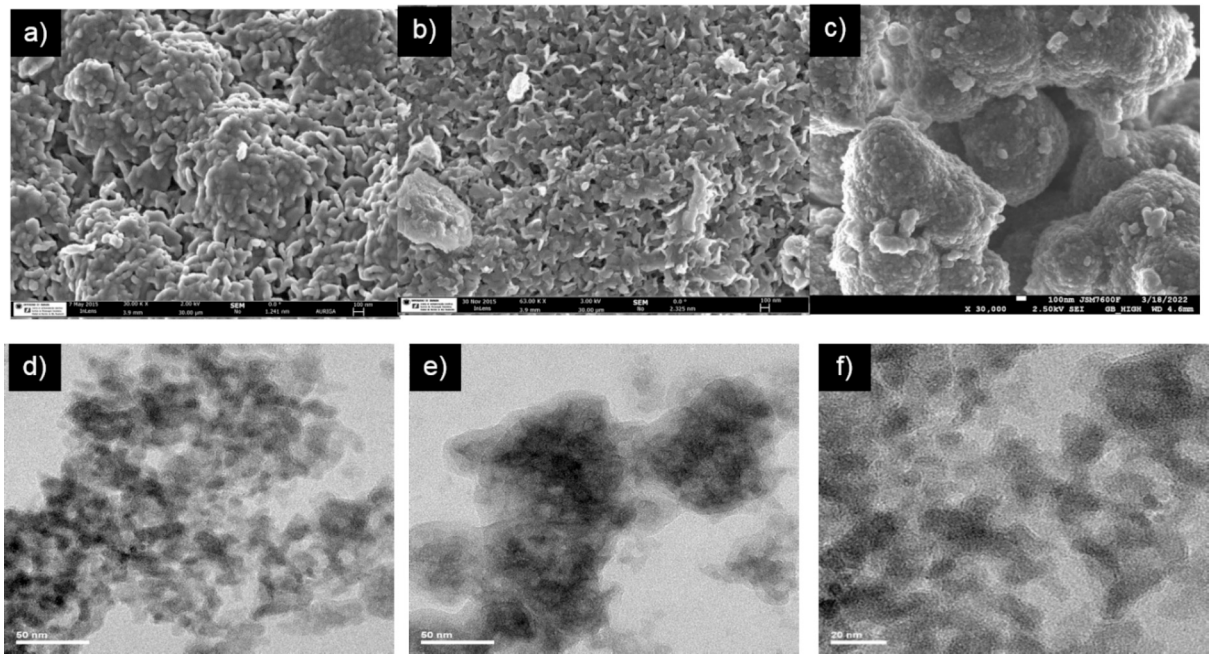

Fig. 5. (a) SEM image of TCeP, (b) SEM image of TCPN, (c) SEM image of TCPH, (d) and (e) TEM and (f) high-resolution TEM of TCPH.

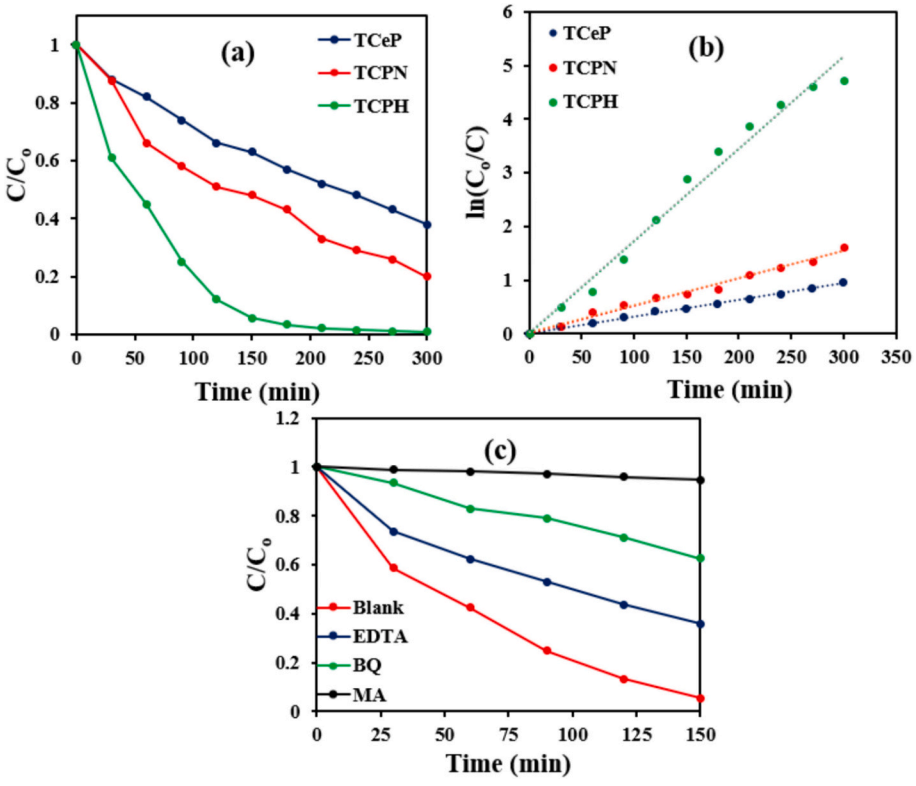

Fig. 6. (a) Photodegradation performance of TCeP, TCPN and TCPH; (b) kinetic model of the photodegradation of MO; and (c) photocatalytic activity of MO over TCPH in the presence of the selected scavengers.

generated radicals and degradation efficiency. The degradation kinetics were studied using a modified Langmuir Hinshelwood model as given in Fig. 6b. The details of the model were previously discussed in our work [37]. The degradation rates were 0.0031, 0.0051 and 0.0172 min^{-1} in the case of TCeP, TCPN and TCPH, respectively. The highest degradation rate was attained in the case of TCPH which is by the results of the comparison between TCeP, TCPN and TCPH.

To get insight into the photocatalytic mechanism over the TCPH and understand the role of the contribution of different generated radicals were investigated using different scavengers such as benzoquinone (BQ, scavenger of superoxide radicals), ethylenediaminetetraacetic acid (EDTA, scavenger of holes) and methanol (MA, scavenger of hydroxyl radicals) at initial MO concentration of 10 mg/L, pH 7, scavengers' concentrations of 20 mM and light intensity of 100 mW/cm^2. The

degradation percentages were 94.45 %, 5.3 %, 64.11 % and 37.5 % in the case of no quencher, MA, EDTA and BQ, respectively (Fig. 6c). The results implied the superiority of the contribution of hydroxyl radicals over other radicals in the degradation process.

3.3. Degradation mechanism

The excitation of coloured defective titania-carbon-phosphorous hybrid composites by LED lamp could contribute to the generation of electron/hole pairs as shown in Fig. 7. The photocatalytic order follows the sequence TCPH >TCPN > TCeP in agreement with the evolution of the band gap values. The better photocatalytic activity than TCPN than TCeP should be associated with the increasing the crystallinity of rutile phase and confirms the importance of the particle size and the interaction with the support. The surface disorder and oxygen vacancies, confirmed from XPS, are the main factors for significant improvement of the charge separation efficiency and subsequently enhance the photocatalytic activity [34]. This observation has been confirmed by the XPS and TEM in Figs. 3 and 5, respectively, In addition, the significantly higher surface area of TCPH results the highest photocatalytic activity.

The electrons would react with oxygen to form superoxide radicals and hydroxyl radicals would be formed via the reaction between holes and hydroxyl ions. The generated superoxide radicals could react with protons to form hydrogen peroxide. However, electrons and holes tend to recombine which decreases the number of generated radicals and reduces the degradation efficiency. The presence of carbon could contribute to the reduction of the recombination rate due to its capability to accept electrons. The electrons might be transferred via carbon to react with the generated hydrogen peroxide to form additional hydroxyl radicals.

In summary, the combination of various factors as increasing the surface area, decreasing the band gap, increasing the localization of surface defects and oxygen vacancies, and higher contributions of the produced hydroxyl radicals, results in a superior photocatalytic activity.

3.4. Reusability of TCPH

TCPH nanoparticles were used in five consecutive photocatalytic cycles and then they were collected after each cycle. Then, the particles were dried in an oven for 24 h for the use in next runs. The degradation ratios were 99.1 %, 98.8 %, 95.7 %, 93.8 and 92.7 % in five repetitive runs at initial MO concentration of 10 mg/L, pH 7, and light intensity of 100 mW/cm^2 as shown in Fig. 8. The partial reduction in the degradation efficiency with the increasing of cycle's number might be due to the coating of binding sites by MO and/or by-products of the photodegradation process which inhibited the production of excessive radicals.

4. Conclusions

Novel surface defect titanium-phosphorous-carbon nanocomposite were prepared by controlled impregnation sol-gel process under controlled atmosphere (N_2 or H_2). In this manner, the oxygen and phosphorous- surface groups formed on cellulose chains during the acid solubilization determine the interactions with the Ti precursor during

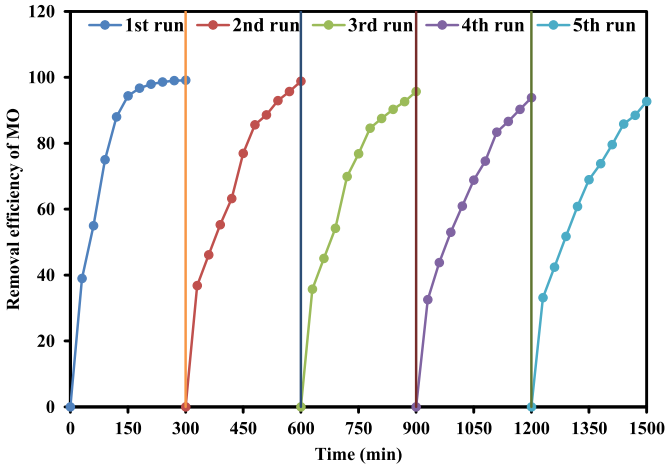

Fig. 8. Removal efficiency of MO under repetitive photocatalytic cycles in the presence of TCPH.

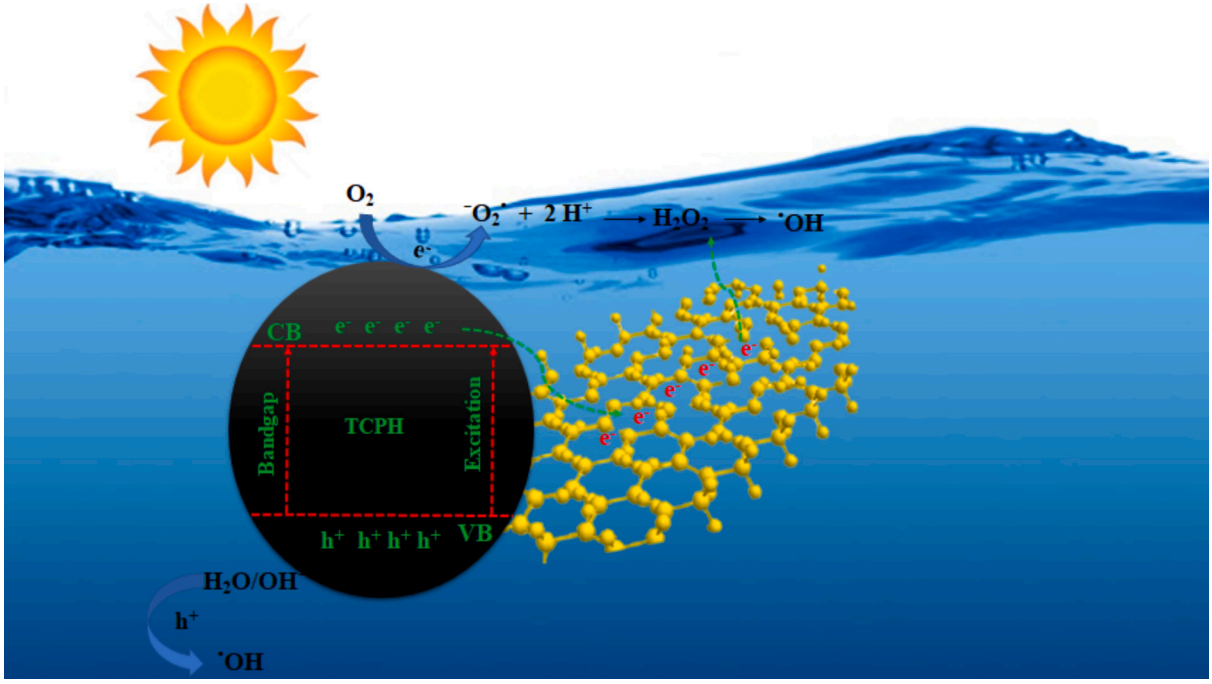

Fig. 7. (a) Proposed degradation mechanism of MO by TCPH.

impregnation as well as the transformations of both cellulose and Ti phases during thermal treatments. Thus, the chemical nature and physicochemical properties of the active phases can be fitted by adjusting the surface chemistry and hydrogenation temperature. The highest degradation rate was attained using TCPH. The hydroxyl radicals were the dominant reactive oxygen species. The boosting photocatalytic behaviour of TCPH could be related to the exceptional physicochemical characteristics such as increasing the Ti^{+3} defects, higher surface area, higher band gap reduction and increasing the probability of the inhibition of electron-hole recombination via formation the carbon. The TCPH could be reused for five repetitive cycles without losing its high catalytic activity. TCPH can be used as a potential catalyst for the degradation of real industrial effluents due to its high degradation performance and stability. Coloured defective carbon-phosphorous-titanium composites offer a new way for the cost-effective degradation of organic pollutants in a large scale as well as open the gate for future fuel generation and light-harvesting energy materials.

CRediT authorship contribution statement

Hesham Hamad: Writing – review & editing, Writing – original draft, Visualization, Validation, Supervision, Software, Resources, Project administration, Methodology, Investigation, Funding acquisition, Formal analysis, Data curation, Conceptualization. **Mahmoud Samy:** Writing – original draft, Visualization, Software, Data curation. **Esther Bailón-García:** Writing – review & editing. **Igor Bezverkhyy:** Writing – review & editing, Visualization, Formal analysis. **Magdalena Skompska:** Writing – review & editing, Visualization. **Francisco Carrasco-Marín:** Writing – review & editing, Supervision, Investigation, Funding acquisition, Conceptualization. **Agustín F. Pérez-Cadenas:** Writing – review & editing, Supervision, Investigation, Funding acquisition, Conceptualization.

Declaration of competing interest

The authors declare that they have no known competing financial interests or personal relationships that could have appeared to influence the work reported in this paper.

Data availability

Data will be made available on request.

Acknowledgements

Hesham Hamad thanks the financial support from MAEC-AECID Spanish fellowship and the Polish National Agency for Academic Exchange (NAWA) for the post-doctoral fellowship within Ulam program (Grant Agreement No. PPN/ULM/2019/1/00149/U/00001). The authors acknowledge the financial support by the Spanish project PID2021-127803OB-I00 funded by MCIN/AEI/https://doi.org/10.13039/501100011033/ and by "ERDF A way of making Europe.", and Grant C-EXP-247-UGR23 funded by Consejería de Universidad, Investigación e Innovación and by FEDER Programa Andalucía 2021-2027. Funding for open access charge: Universidad de Granada / CBUA.

Appendix A. Supplementary data

Supplementary data to this article can be found online at https://doi.org/10.1016/j.ijbiomac.2024.132304.

References

[1] R. Raliya, C. Avery, S. Chakrabarti, P. Biswas, Photocatalytic degradation of methyl orange dye by pristine titanium dioxide, zinc oxide, and graphene oxide nanostructures and their composites under visible light irradiation, Appl. Nanosci. 7 (2017) 253–259, https://doi.org/10.1007/s13204-017-0565-z.

[2] H. Hamad, E. Bailón-García, S. Morales-Torres, F. Carrasco-Marín, A.F. Pérez-Cadenas, F.J. Maldonado-Hódar, Functionalized cellulose for the controlled synthesis of novel carbon-ti nanocomposites: physicochemical and photocatalytic properties, Nanomaterials 10 (2020), https://doi.org/10.3390/nano10040729.

[3] M. Samy, M.G. Ibrahim, M. Fujii, K.E. Diab, M. Elkady, G. Alalm, CNTs/MOF-808 painted plates for extended treatment of pharmaceutical and agrochemical wastewaters in a novel photocatalytic reactor, Chem. Eng. J. 406 (2021) 7, https://doi.org/10.1016/j.cej.2020.127152.

[4] T. Łęcki, H. Hamad, K. Zarębska, E. Wierzynska, M. Skompska, Mechanistic insight into photochemical and photoelectrochemical degradation of organic pollutants with the use of $BiVO_4$ and $BiVO_4$/Co-Pi, Electrochim. Acta 434 (2022) 141292, https://doi.org/10.1016/j.electacta.2022.141292.

[5] Y. Fu, L. Sun, H. Yang, L. Xu, F. Zhang, W. Zhu, Visible-light-induced aerobic photocatalytic oxidation of aromatic alcohols to aldehydes over Ni-doped NH_2-MIL-125(Ti), Appl. Catal. B Environ. 187 (2016) 212–217, https://doi.org/10.1016/j.apcatb.2016.01.038.

[6] S. Mishra, V. Singh, L. Cheng, A. Hussain, B. Ormeci, Nitrogen removal from wastewater: a comprehensive review of biological nitrogen removal processes, critical operation parameters and bioreactor design, J. Environ. Chem. Eng. 10 (2022) 107387, https://doi.org/10.1016/j.jece.2022.107387.

[7] H. Hamad, J. Castelo-Quibén, S. Morales-Torres, F. Carrasco-Marín, A.F. Pérez-Cadenas, F.J. Maldonado-Hódar, On the interactions and synergism between phases of carbon-phosphorus-titanium composites synthetized from cellulose for the removal of the Orange-G dye, Materials (Basel) 11 (2018), https://doi.org/10.3390/ma11091766.

[8] M. Samy, M. Gar, M. Fujii, M.G. Ibrahim, Doping of Ni in MIL-125 (Ti) for enhanced photocatalytic degradation of carbofuran: reusability of coated plates and effect of different water matrices, J. Water Process Eng. 44 (2021) 102449, https://doi.org/10.1016/j.jwpe.2021.102449.

[9] U.S. Meda, K. Vora, Y. Athreya, U.A. Mandi, Titanium dioxide based heterogeneous and heterojunction photocatalysts for pollution control applications in the construction industry, Process. Saf. Environ. Prot. 161 (2022) 771–787, https://doi.org/10.1016/j.psep.2022.03.066.

[10] H. Hamad, M.A. El-Latif, A.E. Kashyout, W. Sadik, M. Feteha, Synthesis and characterization of core–shell–shell magnetic ($CoFe_2O_4$–SiO_2–TiO_2) nanocomposites and TiO_2 nanoparticles for the evaluation of photocatalytic activity under UV and visible irradiation, New J. Chem. 39 (2015) 3116–3128, https://doi.org/10.1039/C4NJ01821D.

[11] U. Sirisha, B. Sowjanya, H. Rehana Anjum, T. Punugoti, A. Mohamed, M. Vangalapati, Synthesized TiO_2 nanoparticles for the application of photocatalytic degradation of synthetic toxic dye acridine orange, Mater. Today Proc. (2022), https://doi.org/10.1016/j.matpr.2022.04.278.

[12] V. Likodimos, A. Chrysi, M. Calamiotou, C. Fernández-Rodríguez, J.M. Doña-Rodríguez, D.D. Dionysiou, P. Falaras, Microstructure and charge trapping assessment in highly reactive mixed phase TiO_2 photocatalysts, Appl. Catal. B Environ. 192 (2016) 242–252, https://doi.org/10.1016/j.apcatb.2016.03.068.

[13] H. Hamad, E. Bailón-García, A.F. Pérez-Cadenas, F.J. Maldonado-Hódar, F. Carrasco-Marín, ZrO_2-TiO_2/carbon core-shell composites as highly efficient solar-driven photo-catalysts: an approach for removal of hazardous water pollutants, J. Environ. Chem. Eng. 8 (2020) 104350, https://doi.org/10.1016/j.jece.2020.104350.

[14] M. Fakhrul Ridhwan Samsudin, S. Sufian, R. Bashiri, N. Muti Mohamed, L. Tau Siang, R. Mahirah Ramli, Optimization of photodegradation of methylene blue over modified TiO_2/$BiVO_4$ photocatalysts: effects of total TiO_2 loading and different type of co-catalyst, Mater. Today Proc. 5 (2018) 21710–21717, https://doi.org/10.1016/j.matpr.2018.07.023.

[15] H. Xia, X. Xu, D. Li, Ligand-decomposition assistant formation of CdS/TiO_2 hybrid nanostructure with enhanced photocatalytic activity, J. Alloys Compd. 914 (2022) 165393, https://doi.org/10.1016/j.jallcom.2022.165393.

[16] A. Hidayat, A. Taufiq, Z.A.I. Supardi, S.M. Jayadininggar, U. Sa'Adah, N. A. Astarini, T. Suprayogi, M. Diantoro, Synthesis and characterization of TiO_2/ZnO-Ag@TiO_2 nanocomposite and their performance as photoanode of organic dye-sensitized solar cell, Mater. Today Proc. 44 (2020) 3395–3399, https://doi.org/10.1016/j.matpr.2020.11.862.

[17] A. Mahana, O.I. Guliy, S.C. Momin, R. Lalmuanzeli, S.K. Mehta, Sunlight-driven photocatalytic degradation of methylene blue using ZnO nanowires prepared through ultrasonication-assisted biological process using aqueous extract of Anabaena doliolum, Opt. Mater. (Amst). 108 (2020) 110205, https://doi.org/10.1016/j.optmat.2020.110205.

[18] M.A. Mohamed, M. Abd Mutalib, Z.A. Mohd Hir, M.F.M. Zain, A.B. Mohamad, L. Jeffery Minggu, N.A. Awang, W.N.W. Salleh, An overview on cellulose-based material in tailoring bio-hybrid nanostructured photocatalysts for water treatment and renewable energy applications, Int. J. Biol. Macromol. 103 (2017) 1232–1256, https://doi.org/10.1016/j.ijbiomac.2017.05.181.

[19] S. Sugashini, T. Gomathi, R.A. Devi, P.N. Sudha, K. Rambabu, F. Banat, Nanochitosan/carboxymethyl cellulose/TiO_2 biocomposite for visible-light-induced photocatalytic degradation of crystal violet dye, Environ. Res. 204 (2022) 112047, https://doi.org/10.1016/j.envres.2021.112047.

[20] Q.C. Liu, D.K. Ma, Y.Y. Hu, Y.W. Zeng, S.M. Huang, Various bismuth oxyiodide hierarchical architectures:alcohothermal-controlled synthesis, photocatalytic activities, and adsorption capabilities for phosphate in water, ACS Appl. Mater. Interfaces 5 (2013) 11927–11934, https://doi.org/10.1021/am4036702.

[21] H. Hamad, E. Bailón-García, S. Morales-Torres, F. Carrasco-Marín, A.F. Pérez-Cadenas, F.J. Maldonado-Hódar, Physicochemical properties of new cellulose-TiO_2 composites for the removal of water pollutants: developing specific interactions

and performances by cellulose functionalization, J. Environ. Chem. Eng. 6 (2018) 5032–5041, https://doi.org/10.1016/j.jece.2018.07.043.
[22] Z. Zhang, C. Zhao, Y. Duan, C. Wang, Z. Zhao, H. Wang, Y. Gao, Phosphorus-doped TiO_2 for visible light-driven oxidative coupling of benzyl amines and photodegradation of phenol, Appl. Surf. Sci. 527 (2020) 146693, https://doi.org/10.1016/j.apsusc.2020.146693.
[23] M. Jiang, M. Zhang, L. Wang, Y. Fei, S. Wang, A. Núñez-Delgado, A. Bokhari, M. Race, A. Khataee, J. Jaromír Klemeš, L. Xing, N. Han, Photocatalytic degradation of xanthate in flotation plant tailings by TiO2/graphene nanocomposites, Chem. Eng. J. 431 (2022), https://doi.org/10.1016/j.cej.2021.134104.
[24] E. Valadez-Renteria, R. Perez-Gonzalez, C. Gomez-Solis, L.A. Diaz-Torres, A. Encinas, J. Oliva, V. Rodriguez-Gonzalez, A novel and stretchable carbon-nanotube/Ni@TiO_2:W photocatalytic composite for the complete removal of diclofenac drug from the drinking water, J. Environ. Sci. (2022), https://doi.org/10.1016/j.jes.2022.05.028.
[25] M. Israr, J. Iqbal, A. Arshad, S.O. Aisida, I. Ahmad, A unique $ZnFe_2O_4$/graphene nanoplatelets nanocomposite for electrochemical energy storage and efficient visible light driven catalysis for the degradation of organic noxious in wastewater, J. Phys. Chem. Solids 140 (2020) 109333, https://doi.org/10.1016/j.jpcs.2020.109333.
[26] H. Hamad, E. Bailón-García, F.J. Maldonado-Hódar, A.F. Pérez-Cadenas, F. Carrasco-Marín, S. Morales-Torres, Synthesis of Ti_xO_y nanocrystals in mild synthesis conditions for the degradation of pollutants under solar light, Appl. Catal. B Environ. 241 (2019) 385–392, https://doi.org/10.1016/j.apcatb.2018.09.016.
[27] Z. Wang, C. Yang, T. Lin, H. Yin, P. Chen, D. Wan, F. Xu, F. Huang, J. Lin, X. Xie, M. Jiang, H-doped black titania with very high solar absorption and excellent photocatalysis enhanced by localized surface plasmon resonance, Adv. Funct. Mater. 23 (2013) 5444–5450, https://doi.org/10.1002/adfm.201300486.
[28] X. Chen, L. Liu, P.Y. Yu, S.S. Mao, Increasing solar absorption for photocatalysis with black hydrogenated titanium dioxide nanocrystals, Science 331 (2011) 746–750, https://doi.org/10.1126/science.1200448.
[29] M.I.G. Miranda, C.I.D. Bica, S.M.B. Nachtigall, N. Rehman, S.M.L. Rosa, Kinetical thermal degradation study of maize straw and soybean hull celluloses by simultaneous DSC–TGA and MDSC techniques, Thermochim. Acta 565 (2013) 65–71, https://doi.org/10.1016/j.tca.2013.04.012.
[30] S. Wei, R. Wu, X. Xu, J. Jian, H. Wang, Y. Sun, One-step synthetic approach for core-shelled black anatase titania with high visible light photocatalytic performance, Chem. Eng. J. 299 (2016) 120–125, https://doi.org/10.1016/j.cej.2016.04.067.
[31] J.M. Rosas, R. Ruiz-Rosas, J. Rodríguez-Mirasol, T. Cordero, Kinetic study of the oxidation resistance of phosphorus-containing activated carbons, Carbon 50 (2012) 1523–1537, https://doi.org/10.1016/j.carbon.2011.11.030.
[32] G. Hasegawa, T. Deguchi, K. Kanamori, Y. Kobayashi, H. Kageyama, T. Abe, K. Nakanishi, High-level doping of nitrogen, phosphorus, and sulfur into activated carbon monoliths and their electrochemical capacitances, Chem. Mater. 27 (2015) 4703–4712, https://doi.org/10.1021/acs.chemmater.5b01349.
[33] J.M. Rosas, J. Bedia, J. Rodríguez-Mirasol, T. Cordero, HEMP-derived activated carbon fibers by chemical activation with phosphoric acid, Fuel 88 (2019) 19–26, https://doi.org/10.1016/j.fuel.2008.08.004.
[34] H. Hamad, M.M. Elsenety, W. Sadik, A. El-Demerdash, A. Nashed, A. Mostafa, S. Elyamny, The superior photocatalytic performance and DFT insights of S-scheme CuO@TiO_2 heterojunction composites for simultaneous degradation of organics, Sci. Rep. 12 (2022) 2217, https://doi.org/10.1038/s41598-022-05981-7.
[35] X. Liu, B. Hou, G. Wang, Z. Cui, X. Zhu, X. Wang, Black titania/graphene oxide nanocomposite films with excellent photothermal property for solar steam generation, J. Mater. Res. 33 (2018) 674–684.
[36] T. Fröschl, U. Hörmann, P. Kubiak, G. Kučerová, M. Pfanzelt, C.K. Weiss, R. J. Behm, N. Hüsing, U. Kaiser, K. Landfester, M. Wohlfahrt-Mehrens, High surface area crystalline titanium dioxide: potential and limits in electrochemical energy storage and catalysis, Chem. Soc. Rev. 41 (2012) 5313–5360, https://doi.org/10.1039/C2CS35013K.
[37] M. Samy, M.G. Ibrahim, M. Gar Alalm, M. Fujii, K.E. Diab, M. ElKady, Innovative photocatalytic reactor for the degradation of chlorpyrifos using a coated composite of ZrV_2O_7 and graphene nano-platelets, Chem. Eng. J. 395 (2020) 124974, https://doi.org/10.1016/j.cej.2020.124974.